Lazar, I. F., Neild, S. A., & Wagg, D. J. (2014). Using an inerter-based device for structural vibration suppression. Earthquake Engineering & Structural Dynamics, 43(8), 1129-1147. 10.1002/eqe.2390

EARTHQUAKE ENGINEERING AND STRUCTURAL DYNAMICS
Earthquake Engng Struct. Dyn. 2010; **00**:1–19
Published online in Wiley InterScience (www.interscience.wiley.com). DOI: 10.1002/eqe

Using an inerter-based device for structural vibration suppression

I. F. Lazar*, S. A. Neild, D. J. Wagg

Department of Mechanical Engineering, University of Bristol, Queen's Building, University Walk, Bristol, BS8 1TR, UK

SUMMARY

This paper proposes the use of a novel type of passive vibration control system to reduce vibrations in civil engineering structures subject to base excitation. The new system is based on the *inerter*, a device that was initially developed for high-performance suspensions in Formula 1 racing cars. The principal advantage of the inerter is that a high level of vibration isolation can be achieved with low amounts of added mass. This feature makes it an attractive potential alternative to traditional tuned mass dampers (TMD). In this paper, the inerter system is modeled inside a multi-storey building and is located on braces between adjacent storeys. Numerical results show that an excellent level of vibration reduction is achieved, potentially offering improvement over TMDs. The inerter-based system is compared to a TMD system by using a range of base excitation inputs, including an earthquake signal, to demonstrate how the performance could potentially be improved by using an inerter instead of a TMD. Copyright © 2010 John Wiley & Sons, Ltd.

Received . . .

KEY WORDS: inerter, structural control, vibration reduction, base excitation

1. INTRODUCTION

Mitigating unwanted vibration in structures is an important part of the design process, particularly for structures which may be subject to seismic excitation. In this paper we propose the use of a novel type of passive vibration suppression control system to reduce vibrations in civil engineering structures based on the *inerter*. The inerter was introduced in the early 2000s by Smith [1] using the force-current analogy between mechanical and electrical networks. The inerter represents the equivalent of the capacitor and has the property that the force generated is proportional to the relative acceleration between its nodes. Its constant of proportionality is called inertance and is measured in kilograms.

Although it was initially used in Formula 1 racing car suspension systems, under the name of J-damper [2], the inerter's application in the field of vibration isolation is much wider today. There are several types of inerters that have already been proposed: the rack and pinion inerter [1], the ball and screw inerter [2] and the hydraulic inerter [3,4]. Experimental testing includes work on car suspensions systems [5,6], while the optimisation of the inerter-based suspension systems is studied in [7]. The optimal performance of the inerter-based vibration isolation systems is discussed in [8–10]. Vehicle suspensions systems employing inerters are discussed in [11], where a mechatronic network strut suspension system is proposed. Inerter-based train suspension systems are studied in [12], while motorcycle steering compensator applications are proposed in [13].

In general, passive vibration control approaches are preferred for civil engineering applications as they avoid the associated stability and robustness issues of active control [14, 15]. Traditional passive control devices include base isolation systems [16–19], TMDs [20,21] and viscous dampers

*Correspondence to: Irina Lazar, Department of Mechanical Engineering, University of Bristol, Queen's Building, University Walk, Bristol, BS8 1TR, UK.

[22–24]. Background information on these systems can be found in [25–27]. The idea of using inerters in base isolation systems for buildings has been recently proposed by [28, 29]. Ikago et al. [30] proposed the use of an inerter-like ball-screw mechanism to be employed in a viscous mass damper (VMD) and a tuned viscous mass damper (TVMD) system. The VMD consists of the inerter-like mass element mounted in parallel with a viscous damper, while the TVMD consists of a VMD mounted in series with an additional spring element. The authors studied the seismic performance of a single-degree-of-freedom (SDOF) structure where the efficiency of a TVMD is assessed in comparison to that of a viscous damper and a VMD. The ball-screw device designed by the authors was capable of generating an apparent mass of 350 kg using a flywheel weighing only 2 kg. Recently, TVMD systems have been installed in a steel structure built in Japan [31]. The control system consists of viscous dampers located between the lower floors and TVMDs located at upper storeys. In [32], the authors present the modal response characteristics of a multiple-degree-of-freedom system incorporated with TVMDs.

In this paper we present a novel control system based on the inerter for suppressing vibrations of civil engineering structures. Given the similarity between an inerter and a mass element, we propose an inerter-based system with a configuration similar to that of a TMD, which we term a tuned-inerter-damper (TID). Accordingly, the inerter is installed in series with spring and damper elements, following the traditional layout of a TMD. However, as the inerter is a two-port device (since it generates a force based on relative acceleration), the TID is connected between storeys as opposed to a TMD which acts on a single storey. TMDs were discussed by Den Hartog in [33] (under the name of dynamic vibration absorbers) with tuning strategies proposed by him and others [34–38]. Based on Den Hartog's guidelines for optimal tuning of TMDs, in this paper we have developed an analogous tuning mehod for a TID.

The TMD performance is limited by the amount of mass that can be added to the original structure. Generally, this does not exceed 10% of the mass of the targeted vibration mode. For inerter devices, gearing allows the effective mass to be far greater than the actual mass of the device. This is commonly achieved using a rack and pinion, however inertial hydraulic devices, with a helical tube providing "gearing", have also been patented [39]. Via this gearing, larger inertance-to-mass ratios can potentially be obtained for TID systems than for TMD ones without an excessive weight penalty and as a result overcoming a major limitation of the TMD. We will show that the performance of inerter-based control systems indicates that they have the potential to be a viable alternative to traditional TMDs.

In Section 2 we introduce a model for the proposed TID vibration supression device and for the building. We also compare the TMD and TID transfer functions. Then in Section 3 we explain how the inerter can be tuned, by considering a SDOF system, which is analogous to the tuning laws developed by Den Hartog. In Section 4 the tuning of a multi-degree-of-freedom (MDOF) system is considered. This includes consideration of a TID system alternatively placed at the bottom and top level of a three-storey building in order to find the configuration offering the best vibration suppression. We finally study the seismic performance of the optimally tuned TMD and TID systems for multi-storey structures. Conclusions are drawn in Section 5.

2. THEORETICAL MODEL

Analogies between mechanical and electrical systems are long established. For example, Firestone [40] discussed the force-current analogy, based on a series of equivalences between elements such as the spring-inductor and damper-resistor equivalence. However, the equivalence between mass elements and capacitors was not complete, because of the fact that one of the mass element's terminals must always be the mechanical ground. The inerter overcomes this limitation and has the property that the force generated is proportional to the relative acceleration between its nodes. Its constant of proportionality is called inertance and is measured in kilograms [1]. The force generated by an inerter is

$$\mathbf{F} = b(\ddot{\mathbf{x}}_i - \ddot{\mathbf{x}}_j) \tag{1}$$

DOI: 10.1002/eqe

where b is the inertance and $\ddot{\mathbf{x}}_i - \ddot{\mathbf{x}}_j$ represents the relative acceleration between the inerter's nodes.

Smith [1] establishes a series of practical conditions that must be fulfilled for the inerter to display satisfactory performance. Most important, the device must have limited mass, regardless of the amount of inertance required and should function in any spatial orientation and motion.

Several types of inerters have been proposed and patented. The most common mechanism consists of a rack, pinions, flywheels and gears. Their number and size is established as a function of the inertance requirements. If we consider a simple device having one rack, a gear of radius r_g and a flywheel with J moment of inertia, the force can be expressed as

$$\mathbf{F} = \frac{J}{r_g^2}(\ddot{\mathbf{x}}_i - \ddot{\mathbf{x}}_j) \tag{2}$$

Therefore, the corresponding inertance is $b = \dfrac{J}{r_g^2}$.

In addition to the relative rather than absolute acceleration dependence, a key feature of the inerter when compared to a mass is the fact that the inertance can be adjusted through gearing, without significantly increasing the inerter's physical mass. Due to this feature, we propose that a TID represents a viable, lower-mass alternative to TMDs — this is assessed by considering a multi-storey building subject to ground excitation.

2.1. Multi-storey building model

The building model is represented by an *n*-storey structure, reduced to a *n*-DOF lumped mass system as shown in Figure 1(a). Two control systems are proposed, a classical TMD and a new type of vibration suppression system formed of an inerter, a spring and a damper — the TID. The control systems are modelled between adjacent storeys and they are shown in Figures 1(b) and 1(c) respectively.

In order to write the equations of motion for the *n*-DOF structure, the storeys are divided in three categories:

(i) the bottom storey, connected to the ground, $i = 1$;
(ii) the i^{th} storey, $i \in [2 : n-1]$;
(iii) the top storey, $i = n$.

The equations of motion for the system in Figure 1 are written in absolute coordinates as

$$\begin{cases} (m_1 s^2 + k_{0,1} + k_{1,2})X_1 = k_{1,2}X_2 + k_{0,1}R + F_{1,0} - F_{1,2} \\ \vdots \\ (m_i s^2 + k_{i-1,i} + k_{i,i+1})X_i = k_{i-1,i}X_{i-1} + k_{i,i+1}X_{i+1} + F_{i,i-1} - F_{i,i+1} \\ \vdots \\ (m_n s^2 + k_{n-1,n})X_n = k_{n-1,n}X_{n-1} + F_{n,n-1} \end{cases} \tag{3}$$

where m_i and $k_{i-1,i}$, $i \in [1 : n]$ represent the mass concentrated on the i^{th} storey and the structural stiffness between storeys $i-1$ and i, respectively; X_i represents the Laplace transform of the i^{th} storey displacement; $F_{i,i-1}$ represents the force exerted by the a control device located between storeys $i-1$ and i on the i^{th} mass and $F_{i,i+1}$ represents the force exerted by the a control device located between storeys i and $i+1$ on the i^{th} mass - see Figure 1. Forces generated by the control devices act at the storey levels, between the floors where they are located. The following sections are dedicated to the study of these forces for both types of control systems and to the computation of structural displacements, using a unified method, regardless of whether the TMD or the TID is employed.

DOI: 10.1002/eqe

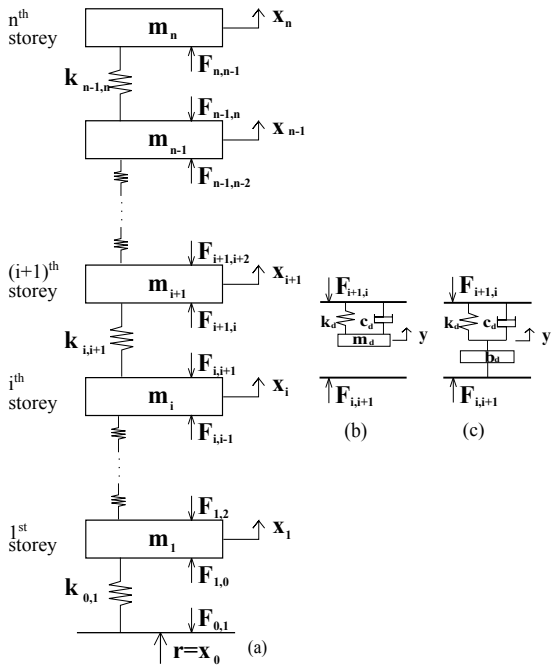

Figure 1. (a) Structural System; (b) TMD system; (c) TID system.

2.2. *TMD vibration suppression system*

We will first study the behaviour of classical TMD systems, and write the generalised expressions of the control forces generated. For the TMD system acting on the i^{th} floor, the control forces can be written in the Laplace domain as

$$F_{i,i+1} = 0 \tag{4a}$$
$$F_{i+1,i} = (k_d + c_d s)(Y - X_{i+1}) \tag{4b}$$

where k_d and c_d are the stiffness and damping of the TMD respectively, X_{i+1} is the Laplace transform of the displacement of m_{i+1} and Y represents the Laplace transform of the TMD mass displacement. Note that we include $F_{i,i+1}$ as it is useful when comparing with the TID device and writing the generalised device equations.

The equation of motion for the y-DOF is given by

$$Y = \frac{c_d s + k_d}{m_d s^2 + c_d s + k_d} X_{i+1} \tag{5}$$

where m_d is the TMD mass. Substituting Equation 5 in Equation 4b it follows that

$$F_{i,i+1} = 0 \tag{6a}$$
$$F_{i+1,i} = -\frac{m_d s^2 (c_d s + k_d)}{m_d s^2 + c_d s + k_d} X_{i+1} \tag{6b}$$

Equations 6a and 6b give the expressions of the control forces obtained when placing a TMD between storeys i and $i+1$, namely $F_{i,i+1}$ and $F_{i+1,i}$ acting on m_i and m_{i+1} respectively.

DOI: 10.1002/eqe

2.3. TID vibration suppression system

If an inerter-based system is mounted at the i^{th} storey level, the control forces can be written in the Laplace domain as

$$F_{i,i+1} = b_d s^2 (X_i - Y) \tag{7a}$$
$$F_{i+1,i} = (k_d + c_d s)(Y - X_{i+1}) \tag{7b}$$

where b_d represents the inertance and X_i represents the Laplace transform of the displacement of mass m_i . The other quantities were defined earlier. Note that now, due to the need for an anchor, the inerter forces are exerted on both the upper and lower storey. The equation of motion for the y-DOF is given by

$$Y = \frac{b_d s^2 X_i + (c_d s + k_d) X_{i+1}}{b_d s^2 + c_d s + k_d} \tag{8}$$

Substituting Equation 8 into Equation 7a it follows that

$$F_{i,i+1} = \frac{b_d s^2 (c_d s + k_d)}{b_d s^2 + c_d s + k_d} (X_i - X_{i+1}) \tag{9a}$$
$$F_{i+1,i} = F_{i,i+1} \tag{9b}$$

Equations 9a and 9b give the expressions of the control forces obtained when placing an inerter-based control system between storeys i and $i+1$, namely $F_{i,i+1}$ and $F_{i+1,i}$ acting on m_i and m_{i+1} respectively. Both forces are non-zero.

2.4. Generalised system

The control forces can be written in a general form, regardless the device used.

$$F_{i,i+1} = l_{i,i+1} T_d d_{i+1} (X_i - X_{i+1}) \tag{10a}$$
$$F_{i+1,i} = l_{i,i+1} T_d (d_{i+1} X_i - X_{i+1}) \tag{10b}$$

where $T_d = \dfrac{\hat{m}_d s^2 (c_d s + k_d)}{\hat{m}_d s^2 + c_d s + k_d}$, $\hat{m}_d = m_d$ or $\hat{m}_d = b_d$ for the TMD and TID respectively. Note that for $i = 0$, $X_0 = R$. In addition, $l_{i,i+1}$ and d_{i+1} are switches that allow us to generalise the device and indicate the location and type of device used respectively. Specifically,

$$\begin{cases} l_{i,i+1} = 1 \text{ , if there is a control device situated between storeys } i \text{ and } i+1 \\ l_{i,i+1} = 0 \text{ , otherwise} \end{cases} \tag{11}$$

and

$$\begin{cases} d_{i+1} = 1 \text{ , if the control system is represented by an inerter between storeys } i \text{ and } i+1 \\ d_{i+1} = 0 \text{ , if the control system is a TMD between storeys } i \text{ and } i+1 \end{cases} \tag{12}$$

Now, we can combine the device(s) by using Equations 10a and 10b to eliminate the control forces $F_{i,i+1}$ from Equation 3. Therefore, we obtain a system of n coupled equations with n unknowns, which are the displacements on each DOF (Equation 13).

$$\begin{cases} X_1 = \dfrac{(k_{1,2} + l_{1,2} T_d d_2) X_2 + (k_{0,1} + l_{0,1} T_d d_1) R}{m_1 s^2 + k_{0,1} + k_{1,2} + l_{0,1} T_d + l_{1,2} T_d d_2} \\ \vdots \\ X_i = \dfrac{(k_{i-1,i} + l_{i-1,i} T_d d_i) X_{i-1} + (k_{i,i+1} + l_{i,i+1} T_d d_{i+1}) X_{i+1}}{m_i s^2 + 2k_{i-1,i} + l_{i-1,i} T_d + l_{i,i+1} T_d d_{i+1}} \\ \vdots \\ X_n = \dfrac{k_{n-1,n} + l_{n-1,n} T_d d_n}{m_n s^2 + k_{n-1,n} + l_{n-1,n} T_d} X_{n-1} \end{cases} \tag{13}$$

DOI: 10.1002/eqe

Note that the displacement of the n^{th} storey depends on the displacement of the storey below only, while the displacement of a middle storey depends on those of the storey bellow and of the storey above. Therefore, if we substitute the expression of X_n from the $(n-1)^{th}$ equation into the n^{th} equation, X_{n-1} will become a function of X_{n-2} only. Successively, following the same procedure, any X_i displacement will depend on X_{i-1} only, for $i = 2...n$. For the bottom storey, we obtain X_1 as a function of R, the ground displacement. After X_1 is computed, all the other displacements are determined.

In order to account for structural damping as well, Equation 13 may be updated by replacing $k_{i,i+1}$ with $k_{i,i+1} + c_{i,i+1}s$, where $c_{i,i+1}$ represents the structural damping between storeys i and $i+1$.

3. TUNING OF THE TID SYSTEM

First we will consider a SDOF system, subjected to sinusoidal ground displacement $r(t) = \sin(\omega t)$. The uncontrolled system is shown in Figure 2(a). The TMD controlled structure is formed combining the systems in Figure 2(a) and 2(b), while the TID controlled structure is formed combining the systems in Figure 2(a) and 2(c).

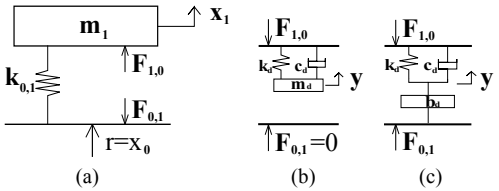

Figure 2. (a) Structural system 1DOF; (b) TMD system; (c) TID system.

The most important aspect in the control system design is the appropriate choice of parameters for all the devices considered. In the case of the TMD systems, optimal tuning rules were established by Den Hartog [33] for a single DOF system, for both undamped and damped vibration absorbers. Den Hartog tuning rules adapted to constant acceleration amplitude base-excited structures (according to [25]) are given below

$$m_d = \mu_m m_1; k_d = \frac{\mu_m}{(1+\mu_m)^2} k_{0,1}; \zeta = \sqrt{\frac{3\mu_m}{8(1+\mu_m)}}; c_d = 2\zeta\sqrt{\frac{k_d}{m_d}} m_d; \tag{14}$$

where m_d, k_d and c_d are the TMD mass, stiffness and damping respectively, and ζ is the TMD damping coefficient. μ_m is the TMD mass ratio, and it is typically chosen in the range $1\% - 10\%$.

Many applications of the inerter have been studied. However, these refer mainly to vibration isolation. Therefore, there are no generally accepted tuning rules suitable for vibration suppression. Smith [1] gives tuning guidelines for inerters used as vibration isolators, specifically in vehicle suspension systems. Such vibration isolation tuning rules do not lead to satisfactory tuning for vibration suppression applications.

Given the similarity between the TMDs and the TIDs, we propose new vibration suppression system tuning rules based on those established for mass-based systems. Den Hartog [33] shows that for an undamped structure, regardless of the choice of TMD stiffness and damping parameters, all displacement response curves in the frequency response diagram pass through two fixed points, P and Q. Moreover, the fixed points location is influenced by stiffness only and is invariant to damping. The frequencies where these points occur are determined analytically, solving a quadratic equation in frequency squared, based on the transfer function between the structural and ground displacements. The stiffness, k_d, is then selected such that the amplitude of response of points P and Q is the same, resulting in the k_d expression in Equation 14. Finally, damping, c_d, is selected such that, through one of these points, the gradient of the displacement response curve is zero — this leads to the damping expression in Equation 14.

DOI: 10.1002/eqe

Following a similar procedure, we firstly show that in the case of TIDs, a third fixed point exists, which we denote as V. Considering the SDOF TID controlled structure, formed by combining the systems in Figure 2(a) and (c), and using Equation 13, the transfer function $X - R$ can be written in the frequency domain as

$$\frac{X}{R}(j\omega) = \frac{k_{0,1} + T_d(j\omega)}{-m_1\omega^2 + k_{0,1} + T_d(j\omega)} \tag{15}$$

where $T_d(j\omega) = \dfrac{-m_d\omega^2(c_d j\omega + k_d)}{-m_d\omega^2 + c_d j\omega + k_d}$ and $j = \sqrt{-1}$. In order to evaluate the response amplitude, the real and imaginary terms are regrouped and Equation 15 is expressed in the form

$$\frac{X}{R}(j\omega) = \frac{A + Bj}{C + Dj}\text{, hence } \left|\left(\frac{X}{R}\right)^2\right| = \frac{A^2 + B^2}{C^2 + D^2} \tag{16}$$

where $A = k_{0,1}k_d - k_{0,1}\omega^2 - b_d\omega^2 k_d$, $B = c_d\omega(k_{0,1} - b_d\omega^2)$, $C = (k_{0,1} - m_1\omega^2)(k_d - b_d) - k_d b_d\omega^2$, and $D = c_d\omega(k_{0,1} - m_1\omega^2 - b_d\omega^2)$. Replacing $b_d = \mu_b m_1$ and $k_d = \alpha\mu_b k_{0,1}$ and regrouping the terms in function of c_d we obtain

$$\left|\left(\frac{X}{R}\right)^2\right| = \frac{(\alpha\mu_b k_{0,1}^2 - \mu_b\omega^2 k_{0,1}m_1 - \mu_b^2\alpha\omega^2 k_{0,1}m_1)^2 + c_d^2\omega^2(k_{0,1} - \mu_b\omega^2 m_1)^2}{[(k_{0,1} - m_1\omega^2)(\alpha\mu_b k_{0,1} - \mu_b m_1\omega^2) - \alpha\mu_b^2\omega^2 k_{0,1}m_1]^2 + c_d^2\omega^2(k_{0,1} - \omega^2 m_1 - \mu_b\omega^2 m_1)^2} \tag{17}$$

where α is a scalar coefficient and $\mu_b = b_d/m_1$ represents the inertance-to-structural mass ratio. Note that μ_b will be referred to as inertance-to-mass ratio. Reformulating,

$$\frac{X}{R} = \sqrt{\frac{E + Fc_d^2}{G + Hc_d^2}} \tag{18}$$

where $E = (k_{0,1}k_d - k_{0,1}b_d\omega^2 - b_d k_d\omega^2)^2$, $F = \omega^2(k_{0,1} - b\omega^2)^2$, $G = ((k_{0,1} - m_1\omega^2)(k_d - b_d\omega^2) - k_d b_d\omega^2)^2$ and $H = \omega^2(k_{0,1} - m_1\omega^2 - b_d\omega^2)^2$.

As our objective is to find the coordinates of fixed points, independent of device damping, c_d, as in Den Hartog's derivation [33], the following condition must be enforced

$$\frac{E}{G} = \frac{F}{H} \tag{19}$$

Solving Equation 19 leads to the following cubic equation in ω^2

$$\mu_b m_1^3\omega^6 - 2(1 + \mu_b + \mu_b\alpha + \mu_b^2\alpha)m_1^2 k_{0,1}\omega^4 + 2(1 + \alpha + 2\mu_b\alpha)m_1 k_{0,1}\omega^2 - 2\alpha = 0 \tag{20}$$

Solutions to Equation 20, giving the frequencies at which the fixed points are located, can be computed — note that for TMDs, the equivalent equivalent equation is a quadratic in ω^2 leading to two damping-invariant points. Solving Equation 20 numerically shows that the first two points are located at low frequencies, situated in the vicinity of the fundamental frequency of the uncontrolled structure and the third point is situated at higher frequencies, where the response has low amplitude. Given the point locations, even though we have three fixed points, the ordinate of the highest frequency fixed point can never exceed those of the two low frequency fixed points. Based on Den Hartog's TMD tuning guidelines, we therefore propose the following TID tuning strategy.

STEP 1 Specify the desired inertance-to-mass ratio, μ_b;

STEP 2 Iterate stiffness, k_d, such that the lower frequency points, P and Q, have equal ordinates. The initial k_d value is based on the TMD tuning rules given in Equation 14;

STEP 3 Find the location of the three fixed points that are independent of damping: P, Q and V. This is done by solving Equation 20;

DOI: 10.1002/eqe

STEP 4 Choose damping, c_d, such that the displacement response has a zero gradient in one of the two low-frequency points, P and Q.

We now present a numerical example. The structure is defined by the following parameters

$$m_1 = 1 \text{ kNs}^2/\text{m}; k_{0,1} = 5000 \text{ kN/m}; \tag{21}$$

such that $\omega_n = 11.25$ Hz. Using the mass ratio $\mu_m = 0.1$, the TMD system parameters used in this application are

$$k_d = 413 \text{ kN/m}; \zeta = 0.18; c_d = 2.37 \text{ kNs/m}; \tag{22}$$

where k_d, ζ and c_d are selected using Equation 14.

The TID system is tuned according to the method explained, following the steps above. Firstly, we chose the inertance-to-mass ratio, $\mu_b = 0.1$, keeping it equal to the TMD mass ratio. Secondly, the stiffness, k_d, is selected such that the lower frequency points, P and Q, have equal ordinates. The TMD tuning rule for k_d given in Equation 14 was used as an initial guess. Therefore, starting from, $k_d = 413$ kN/m, we iterated STEP 2 until we found the value at which points P and Q have equal ordinates, $k_d = 434$ kN/m. Then, the coordinates of the fixed points are determined numerically from Equation 20: $\omega_P = 9.39$ Hz, $\omega_Q = 11.67$ Hz and $\omega_V = 52.83$ Hz. Finally, we calculate the structure frequency response for several damping values shown in Figure 3, from which $c_d = 2.5$ kNs/m is selected as the optimal damping value.

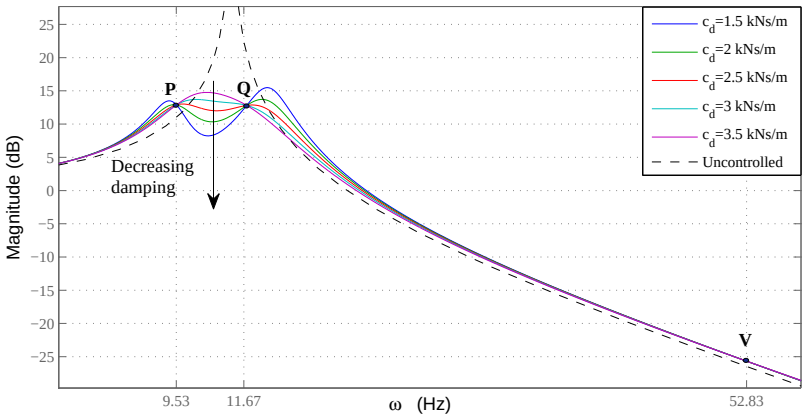

Figure 3. Choice of optimal damping for the TID system for $\mu_b = 0.1$.

Therefore, the numerical values employed are

$$\mu_b = 0.1; k_d = 434 \text{ kN/m}; c_d = 2.5 \text{ kNs/m}; \tag{23}$$

Figure 4 shows the frequency response of the SDOF uncontrolled system, together with that of the TMD and TID controlled systems. It can be seen that the two systems display very similar behaviour near resonance. At high frequencies, the TID system response is very slightly larger than that of the TMD and uncontrolled systems, but the overall response amplitude is small. Each zoom-in represents a comparison of displacement time histories of the TMD and TID systems for $\mu_m = \mu_b = 0.1$.

However, as detailed in Section 2, the inertance-to-structural mass ratio, μ_b, can be set to high values via gearing, as opposed to increased added mass which results in an improved response. Figure 5 , shows the steady state frequency response of the structure for $\mu_b = [0.1; 0.25; 0.5]$ and $\mu_m = 0.1$. As seen, the displacements decrease as μ_b increases. Given the performance of the TID

DOI: 10.1002/eqe

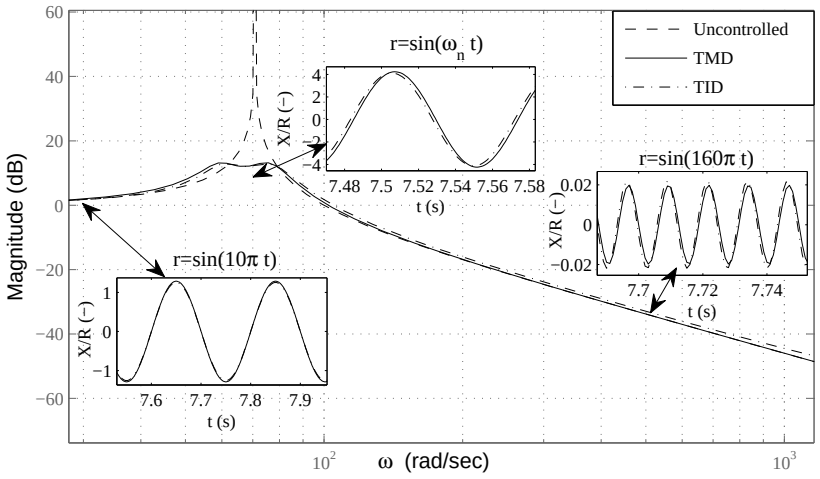

Figure 4. Systems performance comparison for $\mu_m = \mu_b = 0.1$.

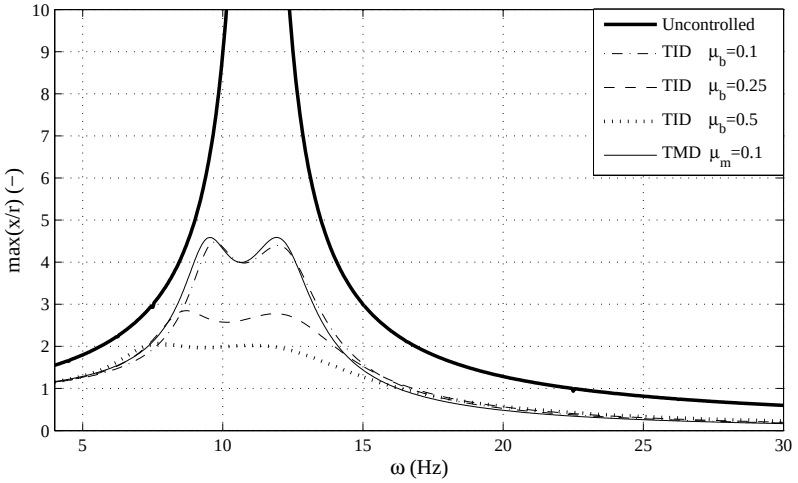

Figure 5. Maximum absolute displacement for $\mu_b = [0.1; 0.25; 0.5]$ and $\mu_m = 0.1$; for $\mu_b = 0.25$, $k_d = 896$ kN/m and $c_d = 8.5$ kNs/m, while for $\mu_b = 0.5$, $k_d = 1333$ kN/m and $c_d = 20$ kNs/m.

controlled system, we can conclude that this represents a viable alternative to TMD devices for 1DOF structures.

The next section is dedicated to the study of a multiple-degrees-of-freedom structure.

4. MDOF SYSTEM

We now consider an n-DOF structure subjected to sinusoidal ground displacement, $r(t) = \sin(\omega t)$. The structure is shown in Figure 1 and described by

DOI: 10.1002/eqe

$$\mathbf{M} = \begin{bmatrix} m_1 & 0 & \dots & 0 \\ 0 & m_2 & \dots & 0 \\ \vdots & \vdots & \ddots & \vdots \\ 0 & 0 & & m_n \end{bmatrix}, \mathbf{K} = \begin{bmatrix} k_{0,1}+k_{1,2} & -k_{1,2} & 0 & \dots & 0 \\ -k_{1,2} & k_{1,2}+k_{2,3} & -k_{2,3} & \dots & 0 \\ 0 & -k_{2,3} & k_{2,3}+k_{3,4} & \dots & \vdots \\ \vdots & \vdots & \vdots & \ddots & -k_{n-1,n} \\ 0 & 0 & \dots & -k_{n-1,n} & k_{n-1,n} \end{bmatrix} \tag{24}$$

In this application, the structural damping is considered equal to zero since its value is typically small compared to the control device damping. Moreover, this choice keeps the structural system similar to the one proposed by Den Hartog.

4.1. Modal analysis — A discussion on TID optimal location

It is well known that TMD systems work more efficiently when located near the top of the structure. This is because the largest displacements generally occur at the top of the structure. We now consider whether the same is true for the TID systems when targeting the first mode of vibration. For this, we analyse the modal response of the controlled structures. The equation of motion for the n-DOF controlled structure, in matrix form, in the Laplace domain is

$$\mathbf{M}s^2Z + \mathbf{K}Z = -\mathbf{M}\begin{bmatrix}1\\1\\\vdots\\1\\1\end{bmatrix}s^2R + \begin{bmatrix} F_{1,0}-F_{1,2} \\ F_{2,1}-F_{2,3} \\ \vdots \\ F_{n-1,n-2}-F_{n-1,n} \\ F_{n,n-1} \end{bmatrix} \tag{25}$$

where $Z = X - R$ represents the vector of relative storey displacements. Although, $\mathcal{L}(\ddot{r}) = s^2\mathcal{L}(r) - sr(0) - \dot{r}(0)$, and for sinusoidal input $\dot{r}(0) = 1$, for this derivation we considered $\mathcal{L}(\ddot{r}) = s^2\mathcal{L}(r) = s^2R$.

Using the transformation $Z = \Phi Q$, where Φ represents the eigenvectors matrix, and pre-multiplying both sides by Φ^T, we obtain

$$\boldsymbol{\mathcal{M}}s^2Q + \boldsymbol{\mathcal{K}}Q = -\Phi^T\mathbf{M}\begin{bmatrix}1\\1\\\vdots\\1\\1\end{bmatrix}s^2R + \Phi^T\begin{bmatrix} F_{1,0}-F_{1,2} \\ F_{2,1}-F_{2,3} \\ \vdots \\ F_{n-1,n-2}-F_{n-1,n} \\ F_{n,n-1} \end{bmatrix} \tag{26}$$

where $\boldsymbol{\mathcal{M}} = \Phi^T\mathbf{M}\Phi$ and $\boldsymbol{\mathcal{K}} = \Phi^T\mathbf{K}\Phi$ represent the modal mass and stiffness matrices respectively.

Using the generalised formulation for the device forces from Equations 10a and 10b and performing the transformation from absolute to relative coordinates, the forces vector on the right hand side can be written as

$$\begin{bmatrix} F_{1,0}-F_{1,2} \\ F_{2,1}-F_{2,3} \\ \vdots \\ F_{n-1,n-2}-F_{n-1,n} \\ F_{n,n-1} \end{bmatrix} = T_d\begin{bmatrix} l_{0,1}(d_1-1) \\ l_{1,2}(d_2-1) \\ \vdots \\ l_{n-2,n-1}(d_{n-1}-1) \\ l_{n-1,n}(d_n-1) \end{bmatrix}R + \dots$$
$$\dots + Td\begin{bmatrix} -l_{0,1}-l_{1,2}d_2 & l_{1,2}d_2 & 0 & \dots & 0 \\ l_{1,2}d_2 & -l_{1,2}-l_{2,3}d_3 & l_{2,3}d_3 & \dots & 0 \\ 0 & l_{2,3}d_3 & -l_{2,3} & \dots & 0 \\ \vdots & \vdots & \vdots & \ddots & \vdots \\ 0 & 0 & \dots & l_{n-1,n}d_n & -l_{n-1,n}d_n \end{bmatrix}\begin{bmatrix} Z_1 \\ Z_2 \\ \vdots \\ Z_{n-1} \\ Z_n \end{bmatrix} \tag{27}$$

DOI: 10.1002/eqe

Note that in the case when TID control systems are used, $d_{i+1} = 1$ and therefore the control forces are independent of the ground displacement, R, as the first term on the right hand side of Equation 27 becomes null.

Now, Equation 27 is considered for each of the four controlled structures and the results are substituted into Equation 26. Then, assuming that only the contribution of the first vibration mode is significant, we obtain the following transfer functions between the modal displacements of the first vibration mode and ground displacement, for each controlled structure.

(i) TMD system located at bottom storey level;

$$\frac{Q_1}{R} = \frac{-\sum_{i=1}^{n}(m_i\Phi_{i,1})s^2 - \Phi_{1,1}T_d}{m_{m1}s^2 + k_{m1} + T_d\Phi_{1,1}^2} \tag{28}$$

(ii) TMD system located at top storey level;

$$\frac{Q_1}{R} = \frac{-\sum_{i=1}^{n}(m_i\Phi_{i,1})s^2 - \Phi_{n,1}T_d}{m_{m1}s^2 + k_{m1} + T_d\Phi_{n,1}^2} \tag{29}$$

(iii) TID system located at bottom storey level;

$$\frac{Q_1}{R} = \frac{-\sum_{i=1}^{n}(m_i\Phi_{i,1})s^2}{m_{m1}s^2 + k_{m1} + T_d\Phi_{1,1}^2} \tag{30}$$

(iv) TID system located at top storey level;

$$\frac{Q_1}{R} = \frac{-\sum_{i=1}^{n}(m_i\Phi_{i,1})s^2}{m_{m1}s^2 + k_{m1} + T_d(\Phi_{n-1,1} - \Phi_{n,1})^2} \tag{31}$$

(v) Damper system located at bottom storey level - This results in a transfer fuction identical with the one in Equations 31.This is because both systems are located at bottom storey level. The difference consists in the control device transfer function, which for a TID is $T_d = \frac{\hat{b}_d s^2(c_d s + k_d)}{\hat{b}_d s^2 + c_d s + k_d}$, while for a viscous damper it is $T_d = c_d s$, where c_d represents damping.

where m_{mi}, $i = 1 \ldots n$ represent the modal masses and k_{m1} is the modal stiffness of the first vibration mode, Φ_{i1} represent the components of the first mode shape, $\Phi_1 = [\Phi_{11}, \Phi_{21}, \ldots, \Phi_{n1}]$, and Q_1 represents the Laplace transform of the displacement of the first vibration mode. Taking into account the fact that $|\Phi_{11}| < |\Phi_{21}| < \ldots < |\Phi_{n1}|$ and analysing the modal displacement-to-ground displacement transfer functions given in Equations 28-31, provided there is no significant modal interaction, it can be seen that:

(i) The fact that the top TMD is more efficient than the bottom one is verified by Equations 28 and 29, since the Φ_{n1}^2 term located at the latter's denominator is much larger than Φ_{11}^2, present in the former equation. Therefore, the modal displacement will be smaller if the TMD is located at the top of the structure;

(ii) Comparing denominators on the right hand side of Equations 29 and 31, we notice that the latter is smaller as it contains a relative term, namely $(\Phi_{n-1,1} - \Phi_{n,1})^2$, while the former is the largest component of the eigenvector, Φ_{n1}^2. Therefore, the system performance is impaired if the same control systems characteristics, contained in T_d, are kept. In order to have identical response on the first mode of vibration we need to scale the TID system according to the ratio $\Phi_{n1}^2/(\Phi_{n-1,1} - \Phi_{n,1})^2$. This has been verified numerically and is shown in the numerical example;

DOI: 10.1002/eqe

(iii) Looking at Equations 30 and 31 it is seen that numerators are identical, while the latter denominator is much lower due to the presence of the relative term. This indicates that the response will be improved if the TID is placed at the bottom storey of the structure. Similarly to (ii), the ratio $\Phi_{11}^2/(\Phi_{n-1,1}-\Phi_{n,1})^2$ indicates that the TID placed at the top of the structure must be over-designed with respect to the TID placed at bottom level in order to obtain identical performance. This has been verified numerically and is shown in the numerical example.

(v) Analysing Equations 28-31 and the remarks above we can conclude that the TID displays a TMD-like behaviour in the vicinity of the first fundamental frequency, due to the similarity between the transfer functions of the two devices. At higher frequencies, we note that $T_d \to c_d$ regardless the type of control system employed (TID, TMD or damper). Therefore, Equations 31 and 32 will lead to the same results if the system is excited in the vicinity of superior resonant frequencies, conferring the TID a damper-like behaviour. This means that the TID combines the advantages of both TMD and damper systems.

4.2. TMD & TID system tuning

The TMD system is tuned according to Den Hartog's guidelines, given in Equation 14, regardless of the device location. These have been adapted to multiple DOF structures, to target the first mode of vibration.

$$m_d = \mu_m m_1; k_d = \omega_1^2 \frac{\mu_m}{(1+\mu_m)^2} m_d; \zeta = \sqrt{\frac{3\mu_m}{8(1+\mu_m)}}; c_d = 2\zeta\sqrt{\frac{k_d}{m_d}} m_d; \tag{32}$$

where ω_1 represents the first fundamental frequency. Please note that the TMD mass is computed as a fraction of m_1, the mass concentrated on one DOF (at one storey level).

The TID system is tuned following the procedure described in 3 and will be detailed in a numerical example in the following subsection.

4.3. Numerical application

All results derived previously, in section 4, are exemplified in a 3-DOF system shown in Figure 6, where $m_1 = m_2 = m_3 = 1\ \mathrm{kNs^2/m}$ and $k_{0,1} = k_{1,2} = k_{2,3} = 1500\ \mathrm{kN/m}$. The numerical values were selected for convenience, while retaining realistic natural frequencies and noting that the parameters scale linearly. As seen in Figure 6, device configurations are considered by modelling each control system (6(b)-6(e)) inside the uncontrolled structure shown in Figure 6(a). Note that only one control system is used at a time.

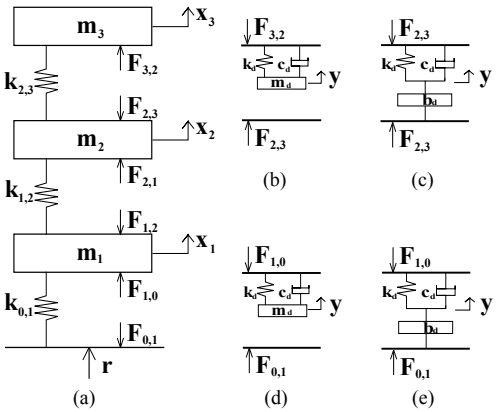

Figure 6. (a) Structural system 3DOF; (b) TMD located at top storey level; (c) TID located at top storey level; (d) TMD located at bottom storey level; (e) TID located at bottom storey level.

The components of the first mode shape, $\Phi_1 = [\Phi_{11}, \Phi_{21}, \Phi_{31}]$ are $\Phi_{11} = -0.328$, $\Phi_{21} = -0.591$ and $\Phi_{31} = -0.737$. We will first study the optimal location of the TID by analysing Equations

DOI: 10.1002/eqe

28 - 31 as described in (ii)-(iii). In this case $(\Phi_{21} - \Phi_{31})^2 = 0.021$, roughly 25 times smaller than $\Phi_{31}^2 = 0.534$. In order to have identical response for top TID and TMD on the first mode of vibration, we need to enforce $\mu_b \approx 25\mu_m$, with the same scaling applied to the TID system's stiffness and damping. This is shown in Figure 7(a). Note that the response curves are not identical since the extra numerator term for the TMD, see Equation 29, has not been taken into consideration. Then, looking at Equations 30 and 31, we notice that $\Phi_{11}^2/(\Phi_{21} - \Phi_{31})^2 \approx 5$ which indicates that in order to obtain identical performance, the TID placed at the top of the structures has to be designed to a capacity that is 5 times larger than that of a TID placed at bottom level. This is shown in Figure 7(b).

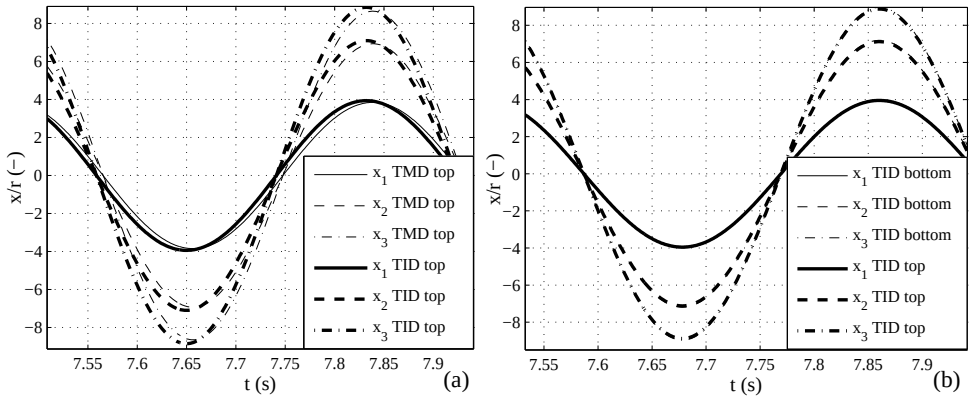

Figure 7. Displacement comparison: (a) TMD top: m_d, k_d, c_d and TID top: $25m_d$, $25k_d$, $25c_d$ and (b) TID bottom: b_d, k_d, c_d and TID top: $5b_d$, $5k_d$, $5c_d$.

Following the remarks above, that have been verified in Figure 7, we conclude that, in contrast to TMDs, placing a TID at bottom storey level is more efficient that placing it at the top. This is a clear advantage of the TID over the TMD as the weight of the device does not need to be supported by the whole structure.

We have analysed the displacement response of all four control systems. The results in Figures 7(a) and 7(b), suggest that in order to obtain similar performance to a TMD located at the top of the structure, a bottom located TID must have roughly 5 times the capacity of the TMD. The inertance-to-mass ratio, μ_b, can have higher values than the TMD mass ratio, μ_m. This is achievable via gearing. The following numerical parameters are proposed for the control systems elements, based on the tuning rules discussed in Section 3. textcolorblue The viscous damper located at bottom storey level was tuned such that it displays similar displacement response with the TID and TMD systems in the vicinity of the first fundamental frequency.

System	μ_b/μ_m	k_d(kN/m)	c_d (kNs/m)
TMD bottom/top	0.03	24.6	1.05
TID bottom	0.15	138.6	2.5
TID top	0.15	158.5	1.5
Damper bottom	-	-	22.5

Table I. Control systems tuning parameters.

The TID and TMD interter-to-mass and mass ratios are computed with respect to the effective mass participating in the first vibration mode. Therefore, the TMD mass ratio is $\mu_m = 3\%$, while the TID inertance-to-mass ration is $\mu_b = 15\%$ of the mass participating in the first mode of vibration. Similar and much higher mass ratios have been used before in TMDs [41] and are much easier to achieve with an inerter due to its gearing. There are several options in choosing the modal mass. Another approach is shown in [43].

DOI: 10.1002/eqe

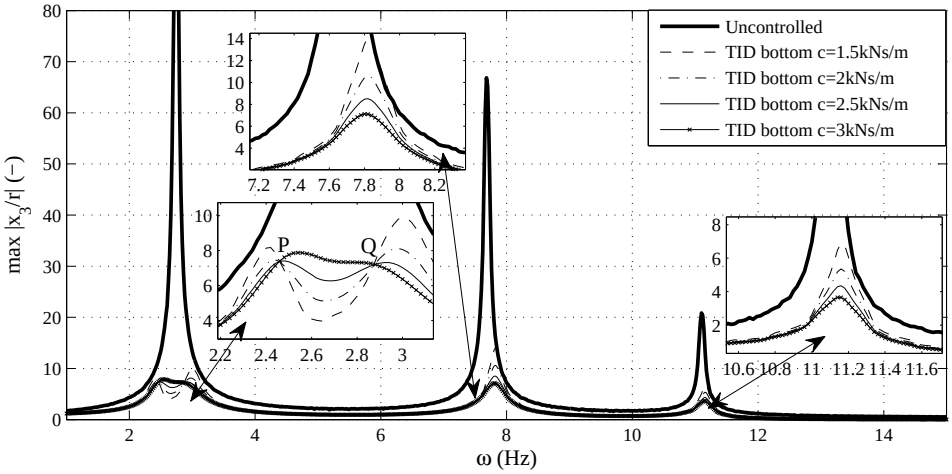

Figure 8. Normalised maximum absolute displacements for TID bottom: $\mu_b = 0.5$, $k_d = 138.6\ \mathrm{kN/m}$ and optimal damping is $c_d = 2.5\ \mathrm{kNs/m}$.

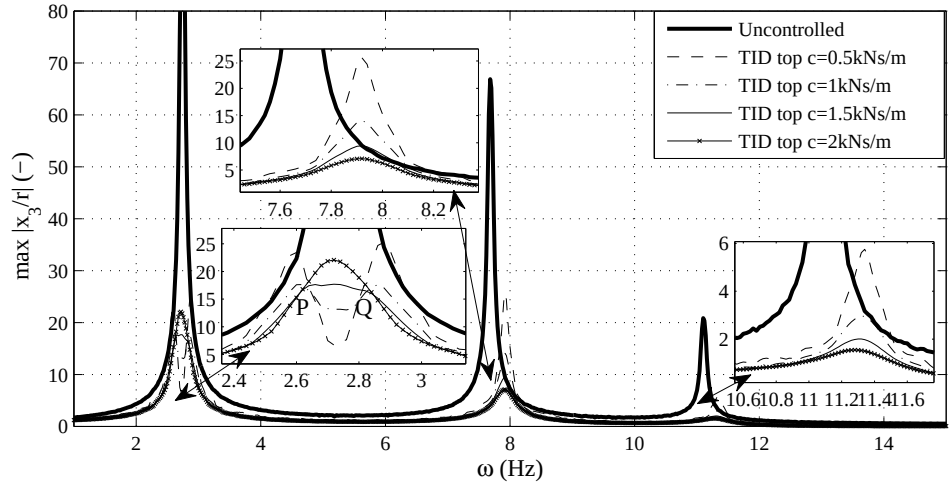

Figure 9. Normalised maximum absolute displacements for TID top: $\mu_b = 0.5$, $k_d = 158.5\ \mathrm{kN/m}$ and optimal damping is $c_d = 1.5\ \mathrm{kNs/m}$.

Figure 8 shows the frequency response in terms of maximum absolute steady-state displacement on the upper DOF for the controlled structure when a TID system is placed at bottom storey level. The first two fixed points, P and Q, are shown in the zoom-in done in the vicinity of the first fundamental frequency of the uncontrolled system. We highlight the points by plotting a range of damping values including the optimal one found using the tuning rules. The other two zoom-ins allow us to observe the structural response in the vicinity of the second and third natural frequencies. The curve that has a horizontal tangent through one of the two fixed points is that obtained when $c_d = 2.5\ \mathrm{kNs/m}$. If damping is further increased, the response is amplified. Similarly, the case when the TID is placed at the top of the structure is shown in Figure 9.

4.4. Performance assessment of TID systems

Figure 10 shows the frequency response of all four TMD and TID control systems, employing the optimal parameters presented in Table I. The best performance is achieved when the TID is placed at lower level, while the TMD in the same location offers the poorest results. If a TMD is placed

DOI: 10.1002/eqe

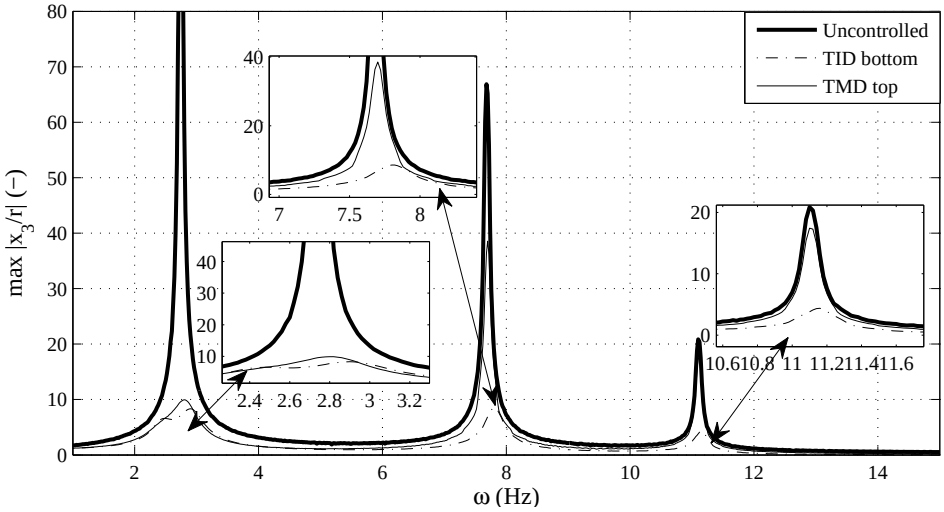

Figure 10. Normalised maximum absolute displacements for $\mu_m = 0.1$ and $\mu_b = 0.5$.

at top storey level, the response obtained is similar to that of the TID placed at the bottom storey level. The response obtained by placing a TID at upper story level is also satisfactory. Also note that the TID systems do not create resonant peaks in the vicinity of the second and third fundamental frequencies, hence the TID is capable of suppressing the response of all three modes, and not only of the one initially targeted, as in the case of TMDs. The inerter or mass-related displacement, y (see Figure 6), has also been evaluated over the same frequency range for the best performing systems, TID located at bottom storey level and TMD located at top storey level. The two systems have similar displacements in the vicinity of the first fundamental frequency, $2.74Hz$. However, in contrast to the TMD, the TID design results in small y-displacement in the vicinity of the second and third fundamental frequencies, $7.7Hz$ and $11.1Hz$ respectively.

For the best performing systems, referred to as TMD top and TID bottom, we calculated the level of the maximum absolute forces in the spring (F_{cd}) and the damper (F_{kd}) and the overall control force (F) for the case when the systems is forced in the vicinity of the first fundamental frequency. These are given in Table II.

System	F_{kd}/r(kN/m)	F_{cd}/r(kN/m)	F/r (kN/m)	stroke$/r$ (-)
TMD top	278	141.8	351	8.99
TID bottom	1513.7	473	1581.6	10.7
Damper bottom	-	1500.5	1500.5	25.54

Table II. Maximum efforts in TMD, TID and damper system elements and overall control forces.

From Table II it can be seen that the spring force is approximately 5.4 times larger for the TID, which is consistent with the ratio between the stiffness of the two control systems. The force in the dampers is 3.3 larger in the case of the TID, while the ratio between their actual damping is 2.4. The overall maximum absolute control force generated by the TID is 4.5 times larger than that generated by the TMD. The control force produced by the damper system is similar to that of the TID system. Please note that if the system is excited at higher frequencies, the damper control force becomes very large in comparison to those of the TID and TMD systems.

The 3 DOF structure has also been subjected to earthquake base excitation. We have chosen a ground acceleration recording from the Tohoku earthquake that took place in Japan on the 11th of March, 2011 which is represented in Figure 11(a).

For this section, the structural damping is no longer kept null, but set to a low damping coefficient of 2%. All other structural parameters are left unchanged, the control systems being tuned optimally

DOI: 10.1002/eqe

(Table I). Figure 11(b) shows the displacement time history on the upper DOF. Three zoom-

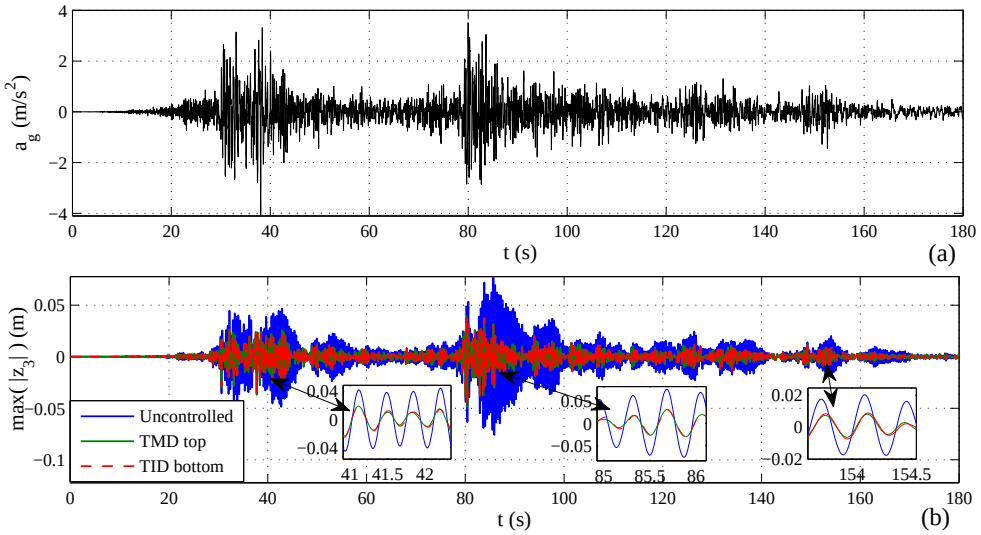

Figure 11. (a)Ground acceleration time-history and (b)Relative displacement time history with 2% structural damping.

in plots are included in the regions where the displacement response is amplified. The results obtained in case of sinusoidal ground excitation are confirmed in case of earthquake excitation. The displacement response obtained with the bottom placed TID is similar to that obtained using a TMD at the top of the structure.

Figure 12(a) shows the single sided Fourier spectrum of the ground acceleration time history. Figure 12(b) shows the single sided Fourier spectra of the displacement response of the uncontrolled structure and the TMD—top location—and TID–bottom location—controlled structures. The highest amplitudes are attained at low frequencies and therefore only the $0 - 8$ Hz frequency range is shown. The first natural frequency of the structure is $\omega_1 = 2.74$ Hz, tuned to match the high amplitude frequency region of the the chosen ground motion. Therefore, the structure is sensitive to the earthquake chosen. The Fourier spectra show the same performance hierarchy.

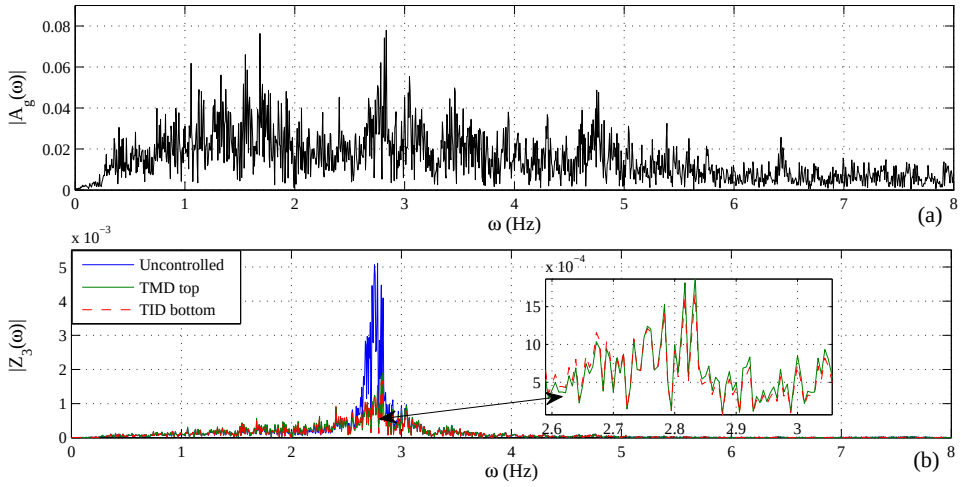

Figure 12. Single sided Fourier spectra: (a) of the ground acceleration and (b) of the displacement response.

DOI: 10.1002/eqe

Since the TID systems behaviour when subjected to earthquake load is satisfactory and very similar to that of TMD systems, we suggest that this new type of control system represents a viable alternative to the traditional TMDs.

4.5. Discussion on TID design for high-rise buildings

In the case of high-rise buildings, the control forces necessary for suppressing unwanted vibrations become larger. We will consider this through an analysis of a 6-DOF and a 10-DOF structure, defined according to Section 4 and employing the same numerical values for m_i and k_i, $i = 1 \dots n$. We will only refer to the best performing systems, the TMD top and TID bottom. Inspecting Equations 29 and 30, we notice that the poles of the two transfer functions are the same provided that the control device transfer fuction, T_d for the TID is scaled by $\phi^2_{n,1}/\phi^2_{1,1}$.

n	1	3	6	10
$\phi^2_{n,1}/\phi^2_{1,1}$	1	5.04	17.2	44.7

Table III. $\phi^2_{n,1}/\phi^2_{1,1}$ ratio for $n = 1, 3, 6, 10$

The ratios $\phi^2_{n,1}/\phi^2_{1,1}$ are given in Table III. This ratio therefore provides an approximate effective inertance-to-mass ratio between the devices — see Section 4. This might appear unfavourable for the TID, but we recall the fact that existing inerter devices built ttain an inertance-to-physical mass ratio of approximately 200 [42] - well above that required here. Therefore, TIDs located at bottom storey level remain a feasible alternative to TMDs.

5. CONCLUSIONS

The paper analyses the possibility of using a TID control system as an alternative to TMDs. The inerter, that has been previously used in vibration isolation applications, is now employed in vibration suppression. First, a generalised framework for computation of the response of TMD and/or TID controlled structures has been developed for n DOF systems. Then, a SDOF structure subjected to sinusoidal base displacement is studied with the intention of deriving a series of tuning guidelines, building on Den Hartog's strategy for TMD systems tuning. It is shown that the TMD and TID systems performance is almost identical when they are tuned at the same mass ratio. However, the inertertance-to-mass ratio can be increased without significantly changing the device physical mass, as inerters are geared. Once this is done, the displacement response is improved. Considering MDOF structures, several TID control system installation possibilities were discussed. The best structural response was obtained with the inerter installed at bottom storey level, connected to the ground. This is beneficial since the control system does not need to be supported by the whole structure anymore. For a better assessment of its performance, the TID was also compared with an equivalent viscous damper located at bottom storey level. The three DOF structure is also subjected to seismic excitation and proves to have similar efficiency to that of TMDs. The small mass and overall size of the device, turns it into an attractive alternative to passive TMDs and damper systems.

ACKNOWLEDGEMENT

The authors would like to acknowledge the support of the EPSRC and the University of Bristol: S. A. Neild is supported by an EPSRC fellowship EP/K005375/1, D.J. Wagg is supproted by EP/K003836/1 and I. F. Lazar is supported by a University of Bristol studentship.

REFERENCES

1. Smith MC. Synthesis of Mechanical Networks: The Inerter. *IEEE Transactions on Automatic Control* 2002; **47**:1648-1662.

2. Chen MZQ, Papageorgiou C, Scheibe F, Wang F-C, Smith MC. The missing mechanical circuit. *IEEE Circuits and Systems Magazine* 2009; **1531-636X**:10-26.
3. Wang F-C, Hong M-F, Lin T-C. Designing and testing a hydraulic inerter. *Proceedings of the Institution of Mechanical Engineers, Part C: Journal of mechanical Engineering Science* 2010, **225**:66-72.
4. Wang F-C, Lin T-C, Hydraulic inerter mechanism, *Patent Application Publication*, No US 2009/0139225A1, 2009.
5. Papageorgiou C, Smith MC, Laboratory experimental testing of inerters. *44th IEEE Conference on Decision and Control and the European Control Conference*. Seville, Spain 2005; 3351-3356.
6. Papageorgiou C, Houghton NE, Smith MC. Experimental Testing and Analysis of Inerter Devices. *Journal of Dynamic Systems, Measurement and Control, ASME* 2009; **131**.
7. Kuznetsov A, Mammadov M, Sultan I, Hajilarov E. Optimization of improved suspension system with inerter device of the quarter-car model in vibration analysis. *Arch. Applied Mechanics* 2011; **81**:1427-1437.
8. Scheibe F, Smith MC, Analytical solutions for optimal ride comfort and tyre grip for passive vehicle suspensions. *Journal of Vehicle System Dynamics* 2009; **47**:1229-1252.
9. Smith MC, Wang F-C. Performance benefits in passive vehicle suspensions employing inerters. *Journal of Vehicle System Dynamics* 2004; **42**:235-257.
10. Wang F-C, Su W-J. Impact of inerter nonlinearities on vehicle suspension control. *International Journal of Vehicle Mechanics and Mobility* 2008, **46**:575-595.
11. Wang F-C, H-A. Chan. Vehicle suspensions with a mechatronic network strut. *International Journal of Vehicle Mechanics and Mobility*, Vol. 49, No. 5, 811-830, 2011.
12. Wang F-C, Liao M-K, Liao B-H, Su W-J, Chan H-A. The performance improvements of train suspension systems with mechanical networks employing inerters. *International Journal of Vehicle Mechanics and Mobility*, Vol. 47, 805-830, 2009.
13. Evangelou S, Limebeer DJN, Sharp RS, Smith MC. Mechanical steering compensators for high-performance motorcycles. *Transactions of the ASME*, Vol. 74, 332-346, 2007.
14. Preumont A. *Vibration Control of Active Structures*, Springer-Verlag, Berlin, 2011.
15. Wagg DJ, Neild SA. *Nonlinear Vibration with Control*, Springer-Verlag, Bristol, 2009.
16. Nagarajaiah S, Sahasrabudhe S. Seismic response control of smart sliding isolated buildings using variable stiffness systems: An experimental and numerical study. *Earthquake Engineering and Structural Dynamics* 2006; **35**(2):177-197.
17. Ordonez D, Foti D, Bozzo L. Comparative study of inelastic response of base isolated buildings. *Earthquake Engineering and Structural Dynamics* 2003; **32**(1):151-164.
18. Malhotra PK. Dynamics of seismic impacts in base-isolated buildings. *Earthquake Engineering and Structural Dynamics* 1997; **26**(5):515-528.
19. Taflanidis AA, Jia GF. A simulation-based framework for risk assessment and probabilistic sensitivity analysis of base-isolated structures. *Earthquake Engineering and Structural Dynamics* 2011; **40**(14):1629-1651.
20. Hoang N, Warnitchai P. Design of multiple tuned mass dampers by using a numerical optimizer. *Earthquake Engineering and Structural Dynamics* 2005; **34**:125-144.
21. Miranda JC. On tuned mass dampers for reducing the seismic response of structures. *Earthquake Engineering and Structural Dynamics* 2005; **34**(7):847-865.
22. Aguirre JJ, Almazan JL, Paul CJ. Optimal control of linear and nonlinear asymmetric structures by means of passive energy dampers. *Earthquake Engineering and Structural Dynamics* 2013; **42**(3):377-395.
23. Lavan O. On the efficiency of viscous dampers in reducing various seismic responses of wall structures. *Earthquake Engineering and Structural Dynamics* 2012; **41**(12):1673-1692.
24. Soong TT, Dargush GF. *Passive Energy Dissipation Systems in Structural Engineering,*, John Wiley & Sons, 1997.
25. Soong TT, Spencer BF Jr. Supplemental Energy Dissipation: State-of-the-Art and State-of-the-Practice. *Journal of Engineering Structures*, Vol. 24, 243-259, 2002.
26. Soong TT, Cimellaro GP. Future directions in structural control. *Structural Control and Health Monitoring*, Vol. 16, 7-16, 2009.
27. Wagg DJ , Neild SA. A review of non-linear structural control techniques. *Proceedings of the Institution of Mechanical Engineers*, Vol. 225, 759-770, 2011.
28. F-C. Wang , C-W. Chen, M-K. Liao, M-F. Hong. Performance analyses of building suspension control with inerters. *Proceedings of the 46th IEEE Conference on Decision and Control*, New Orleans, LA, USA, 3786-3791, 2007.
29. Wang F-C, Hong M-F, Chen C-W. Building suspensions with inerters. *Proceedings IMechE, Journal of Mechanical Engineering Science*, Vol. 224, 1605-1616, 2009.
30. Ikago K, Saito K, Inoue N. Seismic control of single-degree-of-freedom structure using tuned viscous mass damper. *Earthquake Engineering and Structural Dynamics* 2012; **41**:453-474.
31. Sugimura Y, Goto W, Tanizawa H, Saito K, Nimomiya T. Response control effect of steel building structure using tuned viscous mass damper. *15th World Conference on Earthquake Engineering*
32. Ikago K, Sugimura Y, Saito K, Inoue K. Modal response characteristics of a multiple-degree-of-freedom structure incorporated with tuned viscous mass damper. *Journal of Asian Architecture and Building Engineering* 2012; 375-382.
33. Den Hartog JP. *Mechanical Vibrations*, McGraw Hill, 1940.
34. Fujino I, Abe M. Design formulas for tuned mass dampers based on a perturbation technique. *Earthquake Engineering and Structural Dynamics* 1993; **22**:833-854.
35. Moutinho C. An alternative methodology for designing tuned mass dampers to reduce seismic vibrations in building structures. *Earthquake Engineering and Structural Dynamics* 2012; **41**(14):2059-2073.
36. De Angelis M, Permo S, Reggio A. Dynamic response and optimal design of structures with large mass ratio TMD. *Earthquake Engineering and Structural Dynamics* 2012; **41**(1):41-60.
37. Sadeh F, Mohraz B, Taylor AW, Chung RM. A method for estimating the parameters of tuned mass dampers for seismic applications. *Earthquake Engineering and Structural Dynamics* 1997; **22**(6):617-635.

38. Hoang N, Fujino Y, Warnitchai P. Optimal tuned mass damper for seismic applications and practical design formulas. *Engineering Structures* 2008; **30**(3):707-715.
39. Garner BG , Smith MC. *Damping and inertial hydraulic device*, Patent Application Publication, No US 2013/0037362A1, 2013.
40. Firestone FA. A new analogy between between mechanical and electrical systems, *J. Acoust. Soc. Amer.*, vol. 4, 249-267, 1933.
41. De Angelis M, Perno S, Reggio A. Dynamic response and optimal design of structures with large mass ratio TMD. *Earthquake Engineering and Structural Dynamics* 2011; **41**:41-60.
42. Smith MC. The inerter concept and its application. *Society of Instrument and Control Engineers Annual Conference*, Fukui, Japan, 2003.
43. Furuhashi T, Ishimaru S. Mode control seismic design with dynamic mass. *14th World Conference on Earthquake Engineering*

DOI: 10.1002/eqe